

High-resolution NMR field-cycling device for full-range relaxation and structural studies of biopolymers on a shared commercial instrument

Alfred G. Redfield

Received: 11 September 2011 / Accepted: 5 December 2011 / Published online: 27 December 2011
© Springer Science+Business Media B.V. 2011

Abstract Improvements are described in a shuttling field-cycling device (Redfield in *Magn Reson Chem* 41: 753–768, 2003), designed to allow widespread access to this useful technique by configuring it as a removable module to a commercial 500 MHz NMR instrument. The main improvements described here, leading to greater versatility, high reliability and simple construction, include: shuttling provided by a linear motor driven by an integrated-control servomotor; provision of automated bucking magnets to allow fast two-stage cycling to nearly zero field; and overall control by a microprocessor. A brief review of history and publications that have used the system is followed by a discussion of topics related to such a device including discussion of some future applications. A description of new aspects of the shuttling device follows. The minimum round trip time to 1T and above is less than 0.25 s and to 0.002 T is 0.36 s. Commercial probes are used and sensitivity is that of the host spectrometer reduced only by relaxation during travel. A key element is development of a linkage that prevents vibration of the linear motor from reaching the probe.

Keywords Dynamics · Relaxation dispersion · Sample shuttle · Commercial instrument · Motor drive

Introduction

History

For several years we have been developing and evaluating a device (henceforth “shuttler”) that can be wheeled up to a

commercial NMR instrument and be installed within an hour, by a single user-installer (Redfield 2003). It has permitted NMR experiments to be performed using the full capabilities of the commercial instrument for preparation and readout, but with the ability to automatically move the sample during the evolution period to a point, far from the center of the instrument’s magnet, where the magnetic field can be much lower, even nearly zero (Roberts and Redfield 2004a, b, Roberts et al. 2004, 2009; Klauda et al. 2008a; Wang et al. 2008; Clarkson et al. 2009; Sivanandam et al. 2009; Shi et al. 2009; Pu et al. 2009a, b, 2010). The experiments thus performed so far are one- and two-dimensional spin–lattice relaxation (R_1) experiments, although other measurements could be performed in this way.

The term “high-resolution field cycling” is generally meant (Korchak et al. 2010; Diakova et al. 2010) to distinguish this type of cycling from “fast field cycling” without moving the sample. In the latter method a switched-coil magnet is used, with a specialized power supply for more rapid field switching than is generally possible by sample shuttling (Ferrante and Sykora 2004; Sousa et al. 2004). There has been extensive development, including commercial instruments (STELAR s.r.l., Pavia, Italy), using such switched coils for fast field cycling, observing at fields of up to a few T, and switching in the ms range.

Offsetting this advantage is the difficulty of making a useful switched-coil system working above about 2 T, with the result that high resolution is impractical, and sensitivity is low. With our attachment, R_1 can be measured, in a 2D mode if appropriate, at any programmed series of fields lower than that provided by the primary magnet of the spectrometer (hence “Full-Range” in our title), with its full resolution and only relaxation-induced loss of signal. However it cannot be used for samples such as tissues, for

A. G. Redfield (✉)
Biochemistry Department, Brandeis University, Mail stop 009,
Waltham, MA 02154, USA
e-mail: redfield@brandeis.edu

which the relaxation rate is more than about 20 s^{-1} , and the two methods are complementary.

An early pneumatic version of our shuttler was described (Redfield 2003), and a shuttler based on this design is now in reliable operation in the laboratory of T.-h. Huang at the Academia Sinica (Taiwan), built by C. Y. Chou and coworkers (private communication). We have made significant improvements in the shuttle design since our original publication, which are described here. Our research publications have demonstrated some of its novel capabilities, and new insights available via field-cycling methods. While all have been relaxation studies, new structural conclusions have sometimes been deduced from relaxation rates.

The first demonstration of this approach was by (Kerwood and Bolton 1987). Earlier versions that moved a sample downward to a second magnet outside the main magnet have been described (Strombotne and Hahn 1964; Weitekamp et al. 1983). Field-cycling is under investigation for use in NMR imaging (Lurie et al. 2010) and dynamic nuclear polarization (DNP) (Krahn et al. 2010; Pileio et al. 2010; Legget et al. 2010) including use of a motor-driven string. For an excellent review of field cycling see (Kimmich and Estaban 2004).

Our recent interest and work in this area was to a large extent stimulated by extensive measurements on biopolymers and tissues by our former colleague S. H. Koenig and his coworkers and collaborators, using switched-coil cycling (Koenig and Brown 1990). We were inspired to develop a motor/timing-belt-driven shuttler by its earlier use by H.-M. Vieth and coworkers (Grosse et al. 1999). They and others have published many novel applications of the method, largely to physical chemistry, which we do not review here.

Recently we received a description of another approach to shuttling field-cycling NMR (Chou et al. 2011) in which the nearly-traditional shuttle tube used to guide the sample, as in our system, is replaced by a system of mechanical rails, thereby providing space to fit a single lighter timing-belt that extends nearly all the way into the center of the 54 mm bore of a commercial 600 MHz spectrometer. In this way the excessively tall construction that we use for our linear motor is avoided. Much of the discussion in the first sections of the current article may be relevant to this approach as well. It should be seriously considered in the design of future shuttlers.

Overview

We will not repeat, in our later sections, detailed descriptions of many basic features already described in (Redfield 2003). The most important technical improvements we have made since then include (1) the use of a servomotor with belts, pulleys, and a mechanical linkage to land the

sample more gently, yet with a somewhat shortened round-trip time, than did our previous system; (2) use of a microprocessor for overall control to achieve greater versatility and simplicity of hardware; and (3) capability to cycle much more rapidly to fields below 0.065 T by use of a second step of demagnetization using a small extra switched coil. Even greater capability could very usefully be achieved by shared use of any commercial spectrometer operating at a field higher than the 11.7 T field of the instrument available to us, with simple modifications of the shuttler.

The major reasons for making these changes were: (1) To eliminate, as far as possible, protein-denaturing effects that we observed with our previous all-pneumatic shuttler. We still do not fully understand the origin of this denaturation, but expected to eliminate it by the ~ 100 -fold reduction in landing deceleration that we get by a programmed trajectory implemented with a servomotor; (2) To simplify and modernize our system to make it easier to build and to install reversibly; (3) To better measure the relaxation dispersions below about 0.05 T that we have found to be interesting (Roberts and Redfield 2004b; Sivanandam et al. 2009; Pu et al. 2010). The features of our device that differ from previous shuttlers are each not particularly dramatic, but we think our overall approach is useful in terms of cost, availability, and convenience.

Section “**Results**” is intended to indicate the wide-range capability of our module, highlighting our most novel and interesting recent collaborative project (Pu et al. 2010) followed by a brief review of our other application publications. Section “**Discussion**” discusses a wide variety of special topics including some speculative proposals. Section “**Methods**” describes the new details of our shuttler only to the degree that we think needed for the reader to understand its major features. As we did for (Redfield 2003) we expect to web-post¹ further details that we think would be useful for someone who wishes to copy these new features to any extent, including listings of pulse sequences and microprocessor software.

We stress that this device is *simple* compared to many proposed augmentations of NMR instruments. It is the result of nearly a decade of part-time thought, design, fabrication, and assembly by the writer, with the essential help of an excellent machinist, which has uncovered many of our early mistakes that we later corrected. The result is both unexpectedly reliable and versatile. Future designers of such systems will be able to make many improvements but will be able to consider these with full knowledge of our experience.

Figure 1 shows the central part of the shuttler-magnet combination, which towers 3.5 M above the floor of the laboratory. Figure 2 shows the linear motor module, which

¹ <http://www.bio.brandeis.edu/faculty/redfield.html>.

includes an integrated-control servomotor mounted on a heavy base, connected to a shaft and timing belt pulleys driving two vertical belt loops, which are connected by a horizontal clamp-on cross piece. The latter drives a 114 cm downward-directed push rod attached to the sample via a special vibration-isolation loose-coupling module (LCM) down into the center of the 11.7 T magnets (henceforth the main magnet).

The linear motor assembly (Fig. 2) can be lifted, when necessary, by a single person using a human-powered fork-lift (not shown), to rest on Teflon-covered rails attached to a light frame. This frame extends to the floor and surrounds the primary 11.7 T magnet (Fig. 1). The linear motor slides easily on the rails, and can be pushed toward the front part of the frame, away from its working position at the center of the main magnet (Fig. 1), when the spectrometer is being used for conventional non-shuttling spectroscopy. Thus, switching between the shuttling and non-shuttling modes is hardly more complicated than a standard probe change, which is done as usual.

The loose-coupling module slides inside a moderately heavy precision glass shuttle tube (Wilmad) whose inside diameter is 20.3 mm. These components together assure that the standard 5 or 8 mm NMR sample tube slides into the probe without touching its interior. The glass shuttle tube is in two sections inside metal mountings which together extend from just above the top of our stock Varian probe to a point 38 cm above the top flange of the magnet.

The motor can thus lift the sample from the sensitive point of the probe to any point, from near the center of the magnet up to 65 mm above its top flange, where the fringe field is 0.0417 T. Magnetic fields from 0.065 to 11.7 T are reached by programming the motor to stop at the point in the magnet bore where the field is as desired by the user, under microprocessor control. The field vs height in the bore was mapped by use of a commercial Gaussmeter (North Shore).

Fields lower than 0.065 T are reached by shuttling to the point 65 mm above the top-flange of the main magnet, and using microprocessor-controlled air coils to buck the fringe field and its gradient at this point. For this purpose we use a large pair of Helmholtz coils mounted above the 11.7 T magnets, as well as a smaller inner fast-switching coil which produces a field of 0.015 T that can be reversed within milliseconds.

Results

Why shuttle in a commercial instrument?

A quick answer is that it provides a unique window into relaxation at low fields, available to anyone having access to a high-field instrument, with greater versatility and

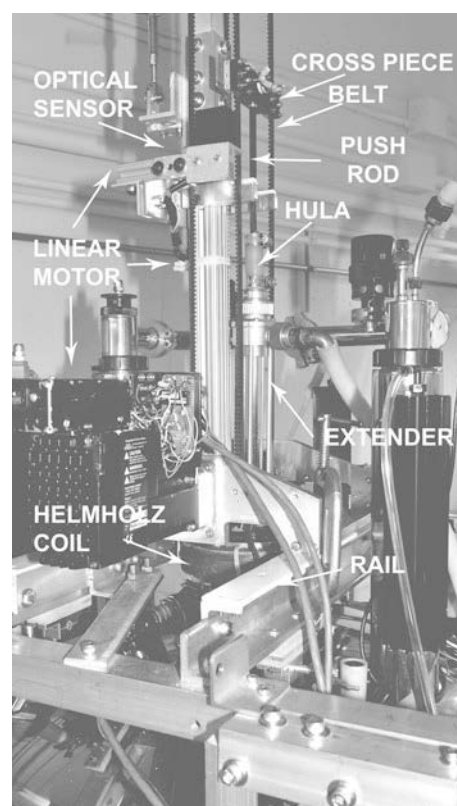


Fig. 1 The shuttler installed on top of the 500 MHz commercial instrument at Brandeis University. The top of one of the four vertical legs of the shuttler support frame is visible in front. They extend to the floor of the laboratory and have height-adjustments at their lower end. The frame of the linear motor is C-clamped to one of the top rails of the frame. Directly between the two timing belts is the extender, containing the short upper section of the glass shuttle tube. Above that can be seen the short piece of gum rubber tubing that is the stomach of the hula bearing. Passing through the hula bearing from the bottom, a short section of the push rod is visible, connected at its top to the black plastic cross-piece which is clamped to the two timing belts. The bottom section of the vertical post, that supports the upper pulleys nearly 1.3 M above, is visible behind the nearest timing belt. The upper of the two Helmholtz coils is visible just below the two rails, covered with white plastic, that support the linear motor assembly. When the shuttler is not used it is pushed to the ends of the rails nearest the camera and re-clamped

sensitivity than earlier approaches (Redfield 2003). We found that this argument did not arouse much interest, even though the utility of relaxation measurements at several different higher fields was already established (Palmer 1997; Koenig and Brown 1990). So we spent several years performing research, in part to demonstrate the utility of this approach, while slowly making technical improvements. We now review our research results so far, mostly very briefly, but with a more extended description of our recent novel methodology and results on membrane dynamics and peripheral membrane proteins.

Below we will use “*reporters*” to denote the nuclear spins whose signals we observe directly or indirectly in the

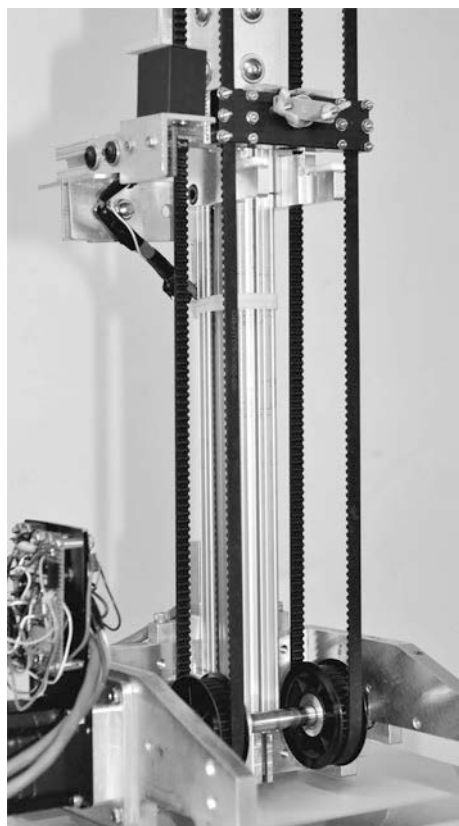


Fig. 2 The linear motor assembly, removed from the frame, to show how straight-forward it is. The front-end of the servomotor is visible on the lower right. The upper ends of the timing belts pass around two smaller pulleys (not shown), which also serve to maintain constant equal tension. The cross-piece is clamped to each of the belts, and in this photograph it is just at the level of the optical-indexing sensor on the left. Behind the servomotor shaft can be seen the heavy rail that extends upward to support the upper two pulleys. The push rod is removed, as it is during tests or when the sample is being changed

high-quality magnetic field of our commercial instrument, and “relaxers” to mean the electronic or nuclear spins species that contribute predominantly to the relaxation rate R_1 of a reporter species via their mutual magnetic dipolar interaction.

All but one of our 12 field-cycling applications papers reviewed below were performed in strong collaboration with M. F. Roberts and her group, at Boston College, complementing the writer’s technical expertise in NMR per se. They have naturally focused on membrane-related problems, reflecting Dr. Roberts’ research interests and expertise. We are enthusiastic about this emphasis because membrane interactions and phospholipid-protein interactions in particular, are continuing to increase in importance and understanding in biology, yet the amount of work on their study using solution NMR has reached a plateau in recent years. These collaborations have also been most valuable for suggesting unique new ways to get basic dynamic and

structural information on the larger aggregates which are now increasingly under scrutiny by NMR and in biology.

Overview of membrane dynamics based on ^{31}P relaxation

At this point we briefly review our results on this topic, partly as an aid to understanding Sect. “Spin labels as relaxers” below.

Figure 3 shows typical early data (Roberts and Redfield 2004a, b) on ^{31}P relaxation in sonicated (25–30 nm diameter) membrane vesicles, of the phosphorus in the phosphodiester linkage that is found in all phospholipids. There have been many NMR studies of the dynamics of the internal alkyl chains of these lipids (Brown et al. 1983; Klauda et al. 2008a; Leftin and Brown 2011) including field-cycling measurements, but not nearly so many on other aspects of membranes (Da Costa et al. 2007; Raschle et al. 2010) such as protein-lipid interactions and dynamics of the head-group phosphodiester region, near the aqueous interface of the membrane surface. One reason for this neglect is that the spectral line of the obvious reporter for this region of the lipid, ^{31}P at the diester linkage, is excessively chemical-shift-anisotropy (CSA) broadened at high magnetic fields.

The reasons that field-cycling phosphorus R_1 measurement is so useful in this context are: (1): the CSA relaxation decreases to be almost negligible at fields below about 3 T; and (2): phosphorus usually has no geminal protons to shorten its T_1 below the upper limit that can be measured in our shuttler, in contrast to amide ^{15}N and aliphatic ^{13}C spins whose R_1 ’s become too high to measure below about 4 T, due to interaction with their geminal protons. In this, as in many biological contexts, phosphorus and/or membranes are of continually increasing importance as targets for NMR study.

The full field dependence of R_1 shown in Fig. 3 was easy to obtain once our apparatus was augmented to reach magnetic fields down to almost zero. No measurements like these had been published previously but the overall interpretation that we now present was obvious once we had the data, and it could have been predicted qualitatively (Lane et al. 1991).

At high field (Fig. 3a, right) CSA relaxation exceeds dipolar relaxation. CSA relaxation could be interesting, and we always measure it carefully because its low field contribution to R_1 is expected to be nearly proportional to the square of the field, so that it can be subtracted from the experimental data at lower fields to get a fair estimate of dipolar relaxation at these fields, that we discuss shortly. The CSA relaxation that is seen at high fields must be due to motions of the four phosphate bonds as a rigid unit. There may also be a lower-field CSA contribution that has

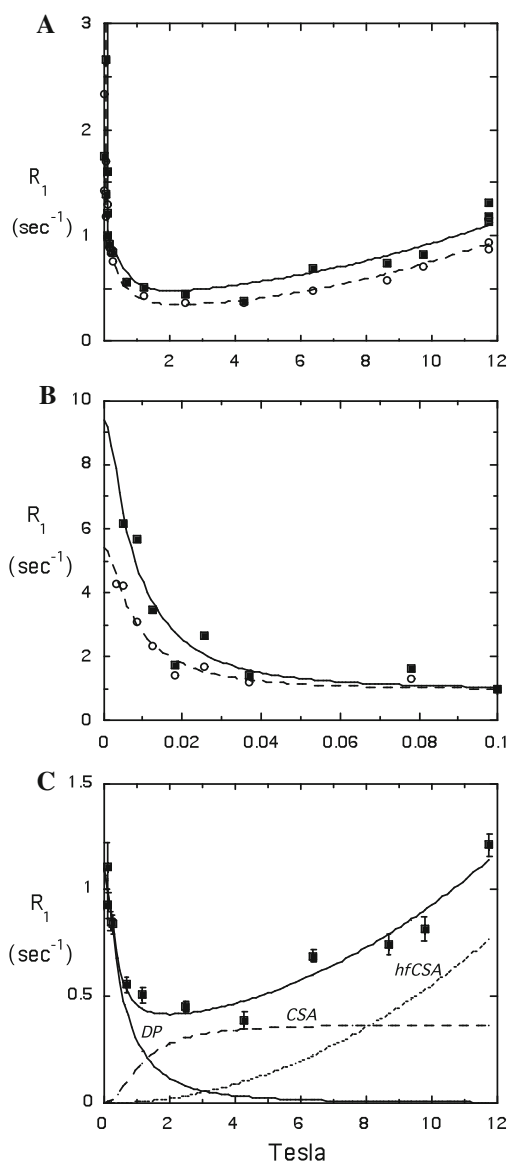


Fig. 3 ^{31}P R_1 data obtained on phospholipid vesicle preparations, phosphatidylcholine (filled square), and phosphatidylmethanol (open circle). **a** Data obtained at all fields on the same samples. **b** Part of the data, obtained at extreme low field. The vertical scale is somewhat compressed, and the horizontal much expanded, compared to part A. The horizontal dotted line is a fit to the flat low-field section of the data points between 0.4 and 0.1 T. The curves are theoretical fits to a single dipolar relaxation prediction based on a Woessner model with an assumed $0.55\ \mu\text{s}$ correlation time. **c** A theoretical fit to the higher-field PC data using minimal parameters: DP, magnetic dipolar relaxation of the ^{31}P spins by surrounding protons; CSA, CSA relaxation from internal motions having the same correlation time as the DP contribution; and hfCSA, CSA relaxation from picosecond dynamics. The latter is similar to the CSA contribution seen in proteins for ^{15}N relaxation. The low-field contribution here marked “CSA” is expected for ^{31}P because of its large CSA interaction, but is predicted to be too small to be significant for ^{15}N in proteins. Single correlation times are assumed for the DP, CSA, and hfCSA curves, and the fits for the latter are not yet based on any suitable detailed dynamic theory. From (Roberts and Redfield 2004b)

hardly been noted theoretically, because it is likely to be negligible compared to dipolar relaxation for other species such as ^{15}N nuclei in amide groups, and is not yet well characterized for ^{31}P .

Figure 3b is an expanded version of the data at the lowest fields, which are not well shown in the wide-field plot of Fig. 3a. Henceforth we will refer to this field range as “very low field”. Had we been studying unsonicated planar membranes whose director is aligned along to the magnetic field, there would have been a residual dipolar splitting of the phosphorus resonance that would be hopelessly small to see at high field, because of CSA broadening. It might be observable at very low field, but not easily, and we have not attempted to do so. If the membrane director were perpendicular to the magnetic field, the splitting would be half as large and the sign of the dipolar interaction would be reversed. In fact, we are studying vesicles tumbling overall on an expected rotational diffusion time-scale of $\sim 1\ \mu\text{s}$. The dipolar interaction averages to zero, but the field-dependence of the relaxation that it produces in the very low field range allows us to estimate its magnitude, and also the rotational diffusion rate of the vesicles. We do so using straightforward fitting of the relaxation data to standard relaxation theory. Thus, the very low-field relaxation dispersion is an indirect measure of the residual dipolar interaction size, and overall tumbling dynamics. This effect is unfortunately an average over all the nearby protons. A better experiment would include a NOESY-style frequency labeling at a field of around 0.05 T, but that would require an extra radio-frequency coil around the shuttle tube, at the position now occupied by the fast-reversing coil.

The very low field dispersion in Fig. 3b is the same one exploited as described in the next section, in connection with our recent spin-label experiments.

Finally, in the mid-to-low field region of Fig. 3a can be seen part of an intermediate-field dispersion whose correlation time, in this and similar vesicles, is about 10–20 ns. This is due to internal dynamics of the vesicle (Fig. 3c), a topic that is often mentioned for proteins but hardly ever studied in detail because the time scale is too short, with a few exceptions such as (Clarkson et al. 2009). Determination of the features of this dipolar dispersion may be complicated by the existence of the lower-field CSA relaxation dispersion just mentioned. There could be a distribution of dispersions within the dipolar dispersion, but they may be difficult to resolve.

Spin labels as relaxers

This topic refers to a subset of the topics usually described as paramagnetic relaxation enhancement, or PRE, reviewed

in (Clare and Iwahara 2009). Our applications are directed toward the same general goal as are PRE measurements, primarily to determine distances between introduced spin labels and interesting reporters. Most previous PRE investigations utilize changes in R_2 of nuclear spin reporters although another subset that could be included uses electron spins as well, as reporters (Borbat and Freed 2007; Batnagar et al. 2010), and could not generally be combined with field-cycling because of the short T_1 of electron spins.

There is only one report, to our knowledge, on PRE with field-cycling measurement of a reporter's R_1 , which we will call PR1E, from the Bryant group (Victor et al. 2005). They also first pointed out the advantage, for field cycling, of what we call “binary PR1E” or BPR1E, which is the case where the reporter and relaxer are attached to different chemical species, and where these two species are weakly bound to each other and dissociate at a rate more rapid than what the PR1E rate would be, if the two species never dissociated. In this case the R_1 that the instrument measures for the reporter is often the weighted average of the free R_1 rate, and the faster rate of the bound form, of the reporter spin. Thus the observed rate can be adjusted, by varying the concentration of the relaxer-carrying species, to be within the rather small range of relaxation rates that our shuttler can measure. The same principle applies, for example, to Michaelis–Menten enzyme kinetics, and to the “transferred NOE” experiment (Clare and Gronenborn 1982), neither of which involve spin labels, of course. For the case of BPR1E with field-cycling it is often possible to estimate the R_1 of free and associated reporters without varying the reporter concentration, as is usually the case for Michaelis–Menten kinetics, because of the fairly well-predictable and different field-variation of the free vs bound rates.

We will now outline the essential features of our most-recently-published collaborative project (Pu et al. 2010) because they are relatively easy to explain, with many elements of similarity to established methods, yet we combining these into an entirely new methodology, with results unobtainable by other methods, as far as we know.

Our major collaborator, Dr. M. F. Roberts, had previously participated in determination of crystal structures of several mutants of the enzyme phosphatidylinositol-specific phospholipase-C (PI-PLC) from *B. thuringiensis*. Comparison to the structure of the closely-related enzyme from *B. cereus* was used to identify a location for the active site of the enzyme, as referenced in (Pu et al. 2010). She also proposed the existence of a separate specific activation site for phosphatidylcholine (PC) on this enzyme to explain the enhancement, by low concentrations of PC, of one of its activities, namely hydrolysis of cyclic inositol-1,2-phosphate (an intermediate of hydrolysis by the enzyme of phosphatidylinositol phosphate (PI) in membranes). PC, incorporated into vesicles of predominantly PI, enhances

activity, consistent with a discrete site for PC binding to the enzyme. Although this proposal was also based to some degree on correlation of the disappearance of the enhancer activity with amino acid substitution, the evidence for a discrete PC site was weak. The data could also be explained as a delocalized electrostatic effect, for example.

PI-PLC is a peripheral membrane protein that is strongly electrostatically-bound to the surface of the membrane (Pu et al. 2009a). There have been no studies, to our knowledge, of such proteins bound to lipid membranes by any structural methods. There have been few previous studies of specific interactions or binding between any membrane proteins and lipids of membrane bilayers (Kang et al. 2010). The crystal structures mentioned above were obtained in the usual way for soluble proteins without the presence of added phospholipids. It was thus not clear whether the crystal structure differed significantly from that of the membrane-bound form of the enzyme.

We had some evidence that the enzyme perturbed the membrane, as might be expected, based on small changes in the membrane dynamics at high added enzyme concentrations that we inferred from our earlier membrane relaxation data (Roberts and Redfield 2004a). It seemed a worthwhile use of our cycling methods to look for a relaxation effect on this ^{31}P lipid resonance produced by single specific spin labels at various sites on the enzyme surface, that did not perturb binding of the enzyme to the membrane as verified by retention of activity. We hoped that such experiments might provide information on the general orientation of the enzyme on the membrane surface. So the Roberts group undertook to make enzyme variants, each with a single cysteine substitution at a specific site; to spin-label them at these sites; and to assay them for full enzyme activity.

When these variants were added to membrane vesicles and ^{31}P field-cycling R_1 measurements were made, they turned out to be potent R_1 relaxing agents at low fields, for the head-group phosphates on the membrane surface, and Dr. Roberts had to find a concentration of enzyme low enough to allow us to measure R_1 over a reasonably informative range of magnetic field (one spin labeled enzyme per 700 lipids, so low that the vesicle surfaces were not nearly saturated with enzyme). The phosphorus R_1 's of two lipids, the activity enhancer PC, and a competitive inhibitor, phosphatidylmethanol (PMe), were studied in sonicated (~30 nm diameter) vesicles containing equimolar amounts of the two lipids. The ^{31}P resonances of the two lipids are well resolved at our readout field of 11.7 T, and it was immediately apparent that the relaxation rates of the two ^{31}P peaks behaved in interestingly different, and most unexpected, ways in response to the added spin label, in contrast to our expectation of rather broad added field dependence reflecting perhaps only a simple orientation effect.

Figure 4 shows examples of the lowest-field dependences of R_1 for the two lipids in three identically sonicated vesicle preparations, to each of which we added the same amount of enzyme, each enzyme spin-labeled at one of three different surface locations. The very low field range shown in Fig. 4 is that for which the overall $\sim 1 \mu\text{s}$ motion dominates, as already shown above in Fig. 3b for vesicles without added enzyme. The dispersions of interest are those below about 0.05 T, which are superimposed on a flat baseline of the low-field end of the dispersions described above at the end of Sect. “Overview of membrane dynamics based on ^{31}P relaxation” that result from motions in the ~ 10 ns time scale. There are small effects on these ~ 10 ns dispersions at much higher concentrations of spin labeled enzyme, but these are negligible at the enzyme concentration used in Fig. 4.

R_1 values for one of these added variants, N220C, denoted by (+) points in Fig. 4, are low for both lipid components, and are similar to their values in the non-spin label samples (Fig. 3b), as expected if the enzyme site N220 is so far from the surface of the membrane, while the enzyme sits on the membrane, as to produce no easily discernable BPR1E on the membrane surface phosphates. Thus, the (+) BPR1E points are an internal control for the R_1 values for the other two samples where an obvious extra BPR1E is seen. They can be subtracted point by point from the rates for enzyme samples with closer spin-labels, to get the purely spin-label BPR1E effect.

When subtraction of the rates found previously for non-spin-labeled enzyme was performed, the data for the combinations of spin label and lipid species that have large BPR1E effects all have a field-dependence that approximates that predicted for a single correlation time in the range of 1–4 μs . The reader can see this by eye-subtraction of the data in Fig. 4b for N220C (+) from that for D205C (\bullet). The same is true for all the other large-amplitude dispersions tabulated in (Pu et al. 2010). They all fall to a rate that is about half the near-zero-field rate, at the same value of field of about 0.01 T. Weaker dispersions like the others in Fig. 4 are consistent with the same range of correlation time, after subtraction of the control data.

The dipolar correlation time for the spin-label contribution to the relaxation is thus the same, approximately, as that for the control experiments, for which its magnitude is explained as resulting from the $\sim 1 \mu\text{s}$ correlation time resulting from overall rotational diffusion time of the vesicles.

The correlation time is generally the time taken for the dipolar interaction, between the reporter and relaxer, to be appreciably changed randomly by dynamics or kinetics in the system. One possibility is that the overall tumbling time of the vesicle might have changed due to the added protein. This is unlikely because the low field dispersion was

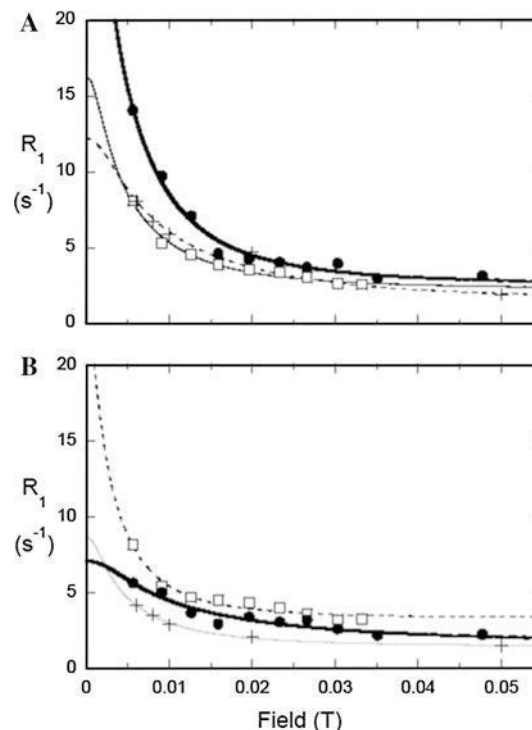


Fig. 4 Very low field relaxation data on three mixed vesicle preparations of 50% each PC and PME (5 mM each). The two lipids have well resolved peaks at the 11.7 T readout field. Data are shown separately for PC (panel A), and PME (panel B). Each sample had a single spin-labeled PI-PLC variant added (14.4 μM). Variants of the PI-PLC are: N220C (+); W47C (open square); D205C (filled circle). From (Pu et al. 2010)

unchanged when we added non-spin-labeled enzyme to the sample at similar concentrations; and is a priori unlikely because of the much smaller mass of enzyme added compared to that of the lipid.

There are two obvious additional mechanisms that would shorten the correlation time for the case of the spin labeled enzyme relaxer sitting on the vesicle surface: the spin-label spins could relax; or the lipid could dissociate from its binding site, while keeping its place on the vesicle surface as it diffuses away from the enzyme (which may likewise diffuse on the surface). Either of these later two rates should add to the widths of the dispersion curves of subtractions data like that of Fig. 4c, if they are comparable to, or larger than, the vesicle’s rotational-diffusion-rate contribution of around 10^6 s^{-1} . But no definite change in this width is seen. It is not surprising that the spin label’s T_1 is more than a microsecond, as appears to be required by this argument.

Of more obvious interest is that the dissociation time of an individual lipid from the site on the enzyme responsible for this dispersion at very low field, *must also be more than around 10^{-6} s*. This time is considerably longer than the time expected for an encounter complex between the lipid and the enzyme, governed by spatial diffusion of an

individual lipid on the vesicle surface. Assuming a 0.5 nm distance d of nearest approach, and a two-dimensional lipid diffusion constant of $D \sim 10^{-7} \text{ cm}^2/\text{s}$ on the membrane surface (Dolainski et al. 1985; Gaede and Gawrisch 2003), the encounter-time would be of order d^2/D , or 25 ns, forty times shorter than the rate we deduce above.

A second feature of the data, in comparing Fig. 3a, b, is that the effects for the two variants other than the control, namely W47C and D205C, are *reversed* for the two panels. W47C is the stronger relaxer for the PMe phosphate in Fig. 3a, while D205C is more potent relaxer for the PC phosphate spin, Fig. 3b. The size of the effect is expected to vary with the inverse sixth power of the distance between the spin label and the phosphate, and the differences seen between the two lipids strongly suggest different predominant binding regions for the two lipids.

These two features together suggest that the two lipids bind at *different specific* sites on the enzyme. Such binding suggests that a given bound lipid is pulled out of the membrane a short distance, perhaps only 0.1 nm or less, where it is bound to the enzyme site for more than a microsecond, and may be either hydrolyzed or else may act as an enhancer, before dissociating.

The Roberts group engineered 8 different cysteine variants of PI-PLC and measured the added effect of spin-labeling the enzymes, on the ^{31}P resonance of the lipids in vesicles for each. Using standard theory, distances for each were estimated for each spin label and the two lipids. The lipid PMe phosphate is considered likely to be an analog of the substrate of the reaction and in the analysis our collaborators placed it at the previously determined active site of the enzymatic reaction. They placed the phosphate of the lipid PC, proposed to be an activity effector, at a likely site about 1.5 nm away from the assumed enzymatic active site. A comparison between distances generated from the X-ray structure under these assumptions and from the NMR experiments, was fair, but at least suggests that the X-ray structure is approximately correct.

Significantly, further experiments described (Pu et al. 2010) using shorter chain lipids, that generally form micelles, not vesicles, were in good agreement with the general picture described above. This unexpected discovery open up a range of further experiments (in progress).

Better data obtained with the new fast-reversing coil, and for a range of enzyme concentrations, may strengthen these conclusions. The computer-aided fits to the spin-label effects do not as yet determine the correlation times very well, but the inferred distance from the spin label to the lipid ^{31}P is almost the same assuming widely different correlations times (1 μs compared to 5 μs), because although the areas under two fitted curves differ by about 20%, the distances inferred from them differ by the differences between the sixth roots of the areas. The problem is not so much to

estimate the distances, but to understand how to interpret the inferred distances correctly given the flexibility of the spin label and the protein (Clore and Iwahara 2009). At the current stage of our data and interpretation, the distance estimates do not allow us to make detailed structural determinations; they serve only as rough tests of the structure, and of the method.

There will be many more cases where cell biologists will want to assay the details of binding, or its existence, to peripheral or integral membrane proteins, or the binding of diverse carrier proteins used to recruit substrates or effectors to membrane enzymes. Procedures similar to the above are likely to be useful in these cases. The method is useful for weak binding, in contrast to most other binding assays. In fact it requires weak binding because it requires a fairly high dissociation rate ($\sim 10^4 \text{ s}^{-1}$ or more) so that the on-enzyme relaxation rate is rate-determining for the overall observed rate.

In conclusion, we turn briefly to another spin-label topic, namely analysis of enzyme active sites using PRE from spin labels attached to a soluble enzyme of interest, close to putative active or inhibitory sites. The reporters are nuclear spins on small molecules that are found to bind to the enzyme of interest without being degraded appreciably. This is difficult for PRE using R_2 of an inhibitor or analog spin as a reporter, because of competing chemical-exchange line-broadening for the reporter on the inhibitor. PR1E also is not useful for this purpose without field-cycling, because the PR1E effect is too small at high field owing to the high resonance frequency of the nuclear spin compared to the inverse of the enzyme's rotational correlation time. This problem is avoided by using field cycling. Our paper (Pu et al. 2009b) shows BPR1E data of this type but goes further by study of the binding in the presence of a micelle which enhances enzyme activity. Paradoxically, the BPR1E experiment seems likely to be easier, the larger is the relaxer-containing species.

This application may be useful for development of good inhibitors (drugs) of larger enzymes, not at the stage of initial screening, but for later refinement where the required cysteine-substituted enzyme variants may already have been made for other reasons. The precise structure of the enzyme under consideration would not need to be known, and the speed limitation on the shuttler would be less serious because the free relaxation rates of the small inhibitors would be much smaller than for the vesicles and proteins that we have studied. Protons could be used as reporters, but spin diffusion during binding, for protons, would have to be well understood and taken into account.

Nucleic acids

Our earliest research paper (Roberts et al. 2004) was our only one on a nucleic acid, and combined a dynamics

simulation by Cui and Case. It indicated that the relatively unexpected CSA relaxation contribution, differing between bases, that we found for ^{31}P in a DNA octamer, was most likely a reporter of sugar pucker variations along the backbone. We will hardly mention nucleic acids again in this paper, but point out that experiments, similar to those we describe herein for proteins and membranes, can be invented to aid in determination of larger distances in nucleic acid structures. These might be based on readily available polynucleotides, including ones attached to spin-labels, and might utilize complementarity with putative unpaired base regions to promote specific binding.

Soluble proteins

(Clarkson et al. 2009) is our only study to date on a soluble protein. We have always been interested in the possible use of our technology to characterize nominally “disordered” regions of proteins. In this case, the region studied (in the N-terminal domain of a coat protein of the simian acute respiratory syndrome virus) turned out, most likely, not to be so very disordered, as suggested by the fact that several successive amide groups within the “disordered” region had the same ~ 1 ns correlation time. It seemed possible, among other things, that the “disordered” region might be a small ordered module that was in motion. This conjecture was supported by a computer simulation of the internal dynamics of the protein. The main data in this paper were obtained using conventional high-field methodology, with low field shuttling relaxation runs only at 7 and 4 T providing support and extra accuracy for the inferred internal ~ 1 ns motion. Relaxation data at a lower field than 4 T was impossible to obtain because the ^{15}N and proton amide spins observed relaxed each other at a rate faster than the speed limitation of our cyclers, below 4 T, as already mentioned in Sect. “[Overview of membrane dynamics based on \$^{31}\text{P}\$ relaxation](#)”. The same limitation is likely for ^{13}C -geminal-proton pairs. Nevertheless we retain our belief that field-cycling will be useful for characterizing nominally disordered regions of proteins, as will be discussed later.

Other membrane topics

Our first membrane paper (Roberts and Redfield 2004a) contained a survey of the ^{31}P relaxation field dependence of a variety of membrane systems, most showing behavior qualitatively like that shown above in Fig. 3. This survey was continued and extended to additives such as cholesterol, and temperature variation in (Roberts et al. 2009). Our early paper (Roberts and Redfield 2004a) included data on a bilayer preparation in which lipids were cross-linked at the lower ends of the alkyl chains, proposed to

support a speculation by the writer concerning the nature of the 10–20 ns as reflecting the rate of rotational diffusion. This conclusion must be viewed with caution because only one preparation could be studied, and the possibility of a phase change could not be ruled out.

Another paper (Roberts and Redfield 2004b) first described the interesting very-low-field dispersion (Fig. 3b) that we observed, in terms of a Woessner model in which the polar angle between the important vectors from the phosphorus to the closest proteins, and the membrane director (which is the vector perpendicular to the average membrane surface), was assumed to be constant. The dominant microscopic relaxation mechanism was assumed to be rotational diffusion of these vectors about the director. Subsequently we have used this model as a convenient way to describe some of our results. However, the supposedly constant angle between P-to-H vectors and the director is, very likely, not constant, and its slower variations (perhaps on the 10–20 ns time scale that our data report) might be significant. The fixed values that we have reported for the polar angle may well be wide-range averages.

Our only study of ^{13}C relaxation in a phospholipid vesicle was of a ^{13}C reporter substituted synthetically on the carbonyl at the internal end of the sn-2 acyl chain of the lipid (Sivanandam et al. 2009). One consequence of these ^{13}C measurements is to support the proposal that measurement of carbonyl relaxation may also be feasible for protein studies down to zero field (see below), in contrast to field-cycling relaxation measurements on ^{15}NH and ^{13}CH pairs (Clarkson et al. 2009). We found almost no high-field CSA relaxation for this carbonyl reporter, but still an intermediate ~ 20 ns dispersion and a moderate very-low-field dispersion like that in Fig. 3b. Interestingly, relaxation data (unpublished) for the same lipid with the ^{13}C reporter on the carbonyl of the other (sn-1) acyl chain show a much more intense very-low-field dispersion, which indicates that the vector, between the carbonyl reporter and the first two acyl protons, is substantially more nearly parallel to the director in the sn-1 location than is the corresponding one for the sn-2 chain.

The paper (Klauda et al. 2008b) is primarily a description of a lengthy and impressive computer simulation of an entire 288-lipid bilayer, by others, compared with experimental results provided by us on a similar vesicle sample at the same temperature. Agreement was excellent for high-field CSA relaxation but the paper was ambiguous concerning overall motion and rotational diffusion of a lipid in a bilayer. These R_1 observations and simulations may convey a sense of confusion about the nature of the 10–20 ns motion that we see in almost all our membrane and micelle systems. This ambiguity is real, and may only be partly dispelled by further relaxation and heteroNOE measurements, and cross-validation with simulations.

The three papers (Wang et al. 2008, Shi et al. 2009, and Pu et al. 2009a) are mainly biochemical studies with minor use of field cycling. However, the first of these was also of special interest to us technically since it was the first instructive reminder of how part-time relatively weak association of a smaller molecule (a short-chain lipid in solution) with a much larger aggregate (a micelle) could be deduced, by observation of a large dispersion in R_1 at very low fields.

So, why shuttle?

Elaborating on our “short answer” to this question above, shuttling is especially useful for studies of larger objects than are often considered by NMR workers to be difficult to handle, such as membranes and protein aggregates, and in cases where structures are not yet well determined. Biological science is advancing to the point where such objects are of increasing interest. Details of both geometry and kinetics might be inferred.

In the case of spin-label PRE, we can determine correlation times over a much shorter time-scale, by measurement of R_1 at fixed fields higher than the spin-locking radio frequency fields available for R_2 dispersion. And R_1 does not have as many confusing interferences, such as chemical exchange-broadening, as exist for R_2 .

The section above has been largely confined our own published papers. Toward the end of the next section we supplement our answer to this question with speculative suggestions of future applications that we are unlikely to be able to attack, due to eventual termination of the current project.

Discussion

Now we list and explain topics that may be more fully elucidated by use of our apparatus, or relevant to its development, including both those for which we have experimental experience, and a few of those for which we do not as yet have, or may never be privileged to have, the pleasure of such experience.

Technical

Why not entirely pneumatic?

After all, it seems much simpler. The main answer is provided in the next paragraph. In addition we repeat that, despite our lengthy description below, and its imposing appearance, the motorized improvement is actually quite simple (Fig. 2), and would undoubtedly be regarded as such by a professional electromechanical engineer. Readers

who are nevertheless reluctant to build the linear motor described in Sect. “Methods” may wish to consider a commercial linear motor such as that mentioned in (Legget et al. 2010) (search www.Festo.com).

Speed limitation of shuttling

The speed limitation was most obvious in (Clarkson et al. 2009), where we studied a ~20 kDa protein with the first motorized version of our system (unpublished) based on a stepper motor. The protein was fully labeled with ^{15}N , and we could only measure the ^{15}N R_1 down to 4 T, below which R_1 became too high for our then-newly-developed motorized shuttler. Because the distances between the relaxer and reporter are well established for these amide pairs and for ^{13}C pairs, limited relaxation measurements on them are still useful for determining contributions to relaxation from motion faster than the overall tumbling rate of the protein, as in this paper. The speed problem is reduced or absent with our current shuttler for reporter species having no geminal protons, like ^{13}C carbonyls (Sivanandam et al. 2009) or carboxyls, as well as phosphates, which do not have geminal protons, or possibly proton methyl groups (Amero et al. 2009), or isolated single protons like adenine C8 protons in a background of deuterons and unlabeled carbons.

For study of soluble proteins with the intention of determining local correlation times (Clarkson et al. 2009) the reporter species might best be one or more ^{13}C labeled peptide carbonyls, with polarization relayed in and out via the nitrogen protons (HNCO) or via the α protons (HACO) before and after the relax-time. This would most likely be the best method to characterize the dynamics of intrinsically disordered regions of proteins.

Another topic relevant to our speed limitation is BPR1E, which is introduced above in Sect. “Spin labels as relaxers”.

Basis as an attachment to a commercial instrument

The previously reported experimental setups for high-resolution field-cycling that are known to us (Korchak et al. 2010; Diakova et al. 2010) have been based on entirely custom-made systems. By attaching to a commercial instrument we save much development time and money, gain versatility, and make the method potentially more accessible to a large number of laboratories at relatively low cost. It would be useful to be able to shuttle on even higher-field instruments for the usual reasons of sensitivity and resolution, and of course to be able to use instruments of any manufacturer. There is no obvious reason why that would not be easily possible with minor modifications of our hardware.

Temperature and deuterium lock

One of the benefits of our parasitic utilization of a commercial instrument is that we do not need to provide a temperature control system within our attachment (Redfield 2003). We think this is because the already-slow rate of thermal equilibration in the instrument is further decreased by the fact that the flow of thermally unregulated air past the sample is very slow when the sample is raised up into the shuttle tube for a few seconds, due to the precise fit of the shuttle to the tube.

We also did not have to build a new lock system. A field-cycle is similar to a “crusher” gradient in its effect on the lock, and the lock system recovers within about 1.5 s after each cycle, during the initial recovery time.

Probe breakage

We bought and use our own Varian probes for fear of breakage of the community probes used by others. Our 10 mm probe was broken catastrophically after about 2 years and was rebuilt in a possibly more rugged form. It has not broken since, in about 6 million cycles, even though we have had a few experiments in which the sample tube broke at the point where it was epoxy-cemented to the adaptor. In these cases the lower part of the sample tube was found sitting inside the undamaged probe, broken from the upper section of the NMR tube, in the region between the seal to the adapter and that to the internal plug. The sample could have been reclaimed. Since we use this 10 mm probe with 8 mm NMR tubes, this good record should be viewed with some reservations. We have used our 5 mm probe, which has never broken using 5 mm tubes, for a much smaller fraction of the time.

A more serious problem arises for shared instruments equipped with the present generation of cryoprobe. Current repair costs of broken cryoprobes are, at least, a psychological barrier for installation of a sample shuttler.

Bubble elimination

We continue to use the same method as fully described in (Redfield 2003), to eliminate motion-induced bubbles, of sealing samples with epoxy cement, below a long hollow plastic insert, for every run. This is not the only proposed way to eliminate bubbles for shuttling (Victor et al. 2004; Chou et al. 2011). Finding a solution to the bubbling problem is an important part of the establishment of any shuttling field-cycling laboratory.

Inhomogeneity of the fringe field

The effect of the huge and unavoidable inhomogeneity at higher fields inside the magnet bore (as great as 1 T across

the 15 mm length of the detected part of the sample) is not expected to affect our overall scientific conclusions in any important way, although we have to keep it in mind.

“Shielded” magnets

Our 500 MHz magnet is unshielded. In some cases use of the now-standard shielded magnets could present problems. For example, if the field reverses at any point along the trajectory of the sample, the relevant nuclear magnetization might not be preserved during passage. This problem might be mitigated by use of a switched solenoid in the upper end of the magnet bore (Ivanov and Redfield 2004).

Physical enhancements, minor and major, and dynamic nuclear polarization

The Vieth group has homogenized the low-field region of their system (analogous to the region 65 mm above the top flange of our magnet), sufficiently well to observe interesting level-crossing effects in small molecules. Our provision of only three copper coils in the region just above the main magnet, one Helmholtz pair for field-bucking and the third one for high-speed field-switching, is primitive. Designers of future shuttle systems should plan to have mechanical supports in this region, between the top of the central magnet and the bottom of the linear motor, for easy substitution of as-yet unplanned optional enhancements. It is probably too difficult to combine all possible enhancements in one space. Different arrays of coils could perform a number of enhancements. These could include a simple system like ours; a better one as installed by the Vieth group; a more powerful fast-switched coil like those developed by STELAR (above); and a DNP test facility, probably with microwave capability (below).

Managers of major facilities which do not have ^{31}P capability at high field should consider buying probes for this purpose; we have found it difficult to locate facilities that do. Those who are designing a resistive or hybrid high-field magnet facility should be so kind as to be able to move the high-resolution magnet used for shuttling directly beneath a hole in the ceiling, to permit shuttling up to the resistive higher-field magnet.

We are reluctant to discuss DNP, because the current article is directed almost solely to providing an inexpensive and simple way to access a range of very useful measurements. Many current DNP methods use added paramagnetic reagents, which could interfere with the low-field dispersion determination that has been so useful to us; and microwave heating would most likely interfere with meaningful study of kinetic rates and activation energies. However, DNP can be used at lower polarization fields to

diagnose properties of materials (Hecht and Redfield 1963) without any major interest in increased signal strength. DNP methods, using polarizing fields of 0.1 to several T, and shuttling the sample down into a ~800 MHz commercial spectrometer, may find a niche compared to those now using a single probe for polarization and readout, because of lower cost, and less crowding with greater flexibility.

Shuttling systems like ours would be useful, as similar systems now are (Krahn et al. 2010; Pileio et al. 2010; Legget et al. 2010) for investigating the feasibility of DNP methods. To this end, we make the following suggestions: (1) Stirring the sample during DNP might be useful to spread the DNP, localized by skin effect, within the volume of a ~5 mm NMR tube. Our current shuttler could shake the sample up and down with only trivial additional programming, and it would be easy to add a small servomotor at the upper end of the push rod, to stir the sample with back-and-forth rotary motion at its highest point of travel. Its stator would be fixed, and its rotor attached to the upper end of the push rod. (2) The long precision-glass shuttle tube that we now use does not have to extend through the DNP-producing assembly. Only 3 or 4 vertical vanes at a radius slightly greater than the shuttle diameter are needed as guides. These could each have loop resonators embedded in them to apply the high frequency power. The open construction of the resonators could allow better cooling of the NMR sample by air jets. (3) There is a possibility that the “solid-effect” DNP method, invented by Abragam and by Jeffries, could be performed in colloidal solutions using spin labels engineered onto surfaces of slowly tumbling large objects. An affinity-based binding site, for the macromolecule being studied, could be engineered about 1 nm away from the spin label. As far as we can see the main question is the limitation in polarization due to saturation of the electron spin by the off-resonance polarizing field. This problem might be mitigated by a time-shared pulsed approach.

Applications

Comparison with computer simulations of internal motion, and hetero-NOE

The kinds of studies described above would best be carried out in conjunction with computer simulation of molecular dynamics in the same region of the protein, for cross-validation and to suggest further experiments. Three of our 12 research publications have included dynamic simulations by collaborators, all with interesting results, in our opinion (Roberts et al. 2004; Klauda et al. 2008b; Clarkson et al. 2009). All involve characterization of what would be called internal motion if proteins were being studied, as was

actually the case for (Clarkson et al. 2009). Internal motions are routinely characterized in soluble proteins by use, especially, of hetero-NOE at fixed field, but, almost always, only to locate flexible regions in the sequence without further characterization. Our applications of field-cycling already exceed, in variety, those which have been used for elucidation of the faster internal motions of proteins. Extending these methods to soluble proteins, to get more information, even using field cycling, will be difficult because of the dominance of the rather simple CSA relaxation mechanism at high fields, and the unavailability of fields above ~20 T. However, something might be learned along the lines we have already demonstrated.

Elucidation of otherwise unobservable complexes

This topic is actually old since the experiment “transferred nuclear Overhauser effect” is in this class (Clare and Gronenborn 1982). As mentioned above, (Wang et al. 2008) was our first unexpected reminder of these possibilities, using the fact that a smaller species which spends a small fraction of its time complexed to a larger one will, under certain kinetic conditions, exhibit a marked dispersion at low field with a rotational correlation time equal to that of the complexed species. In some cases binding constants are obtained (Pu et al. 2009b) in this way, or limits on them can be inferred (Pu et al. 2010). This is a large complicated topic and we cannot treat it properly here. It is especially important for ^{31}P reporters where CSA broadening limits the utility of high-field-only experiments, such as the Carr-Purcell-Mieboom-Gill sequence, that are useful for species such as protons or ^{15}N . We think that this aspect of our work is especially important, given the tremendous importance of phosphorus in biology.

Paramagnetic relaxers

We already described PRE experiments using spin-labels. Paramagnetic ions bound by thiol-based chelators may also be useful (Clare and Iwahara 2009). Many paramagnetic ions have exceedingly high electron spin–lattice relaxation rates (R_{1e} 's). For these the “Boltzman moment” approximation would apply (Gueron 1975), and their major PRE effect would decrease at low field (in close analogy to nuclear spin CSA relaxation), rather than increase, making them relatively useless for field cycling. The only useful ionic paramagnetic species in the context of field-cycling are thus likely to be the high-spin ions of Mn^{+2} , and perhaps Cu^{+2} and Gd^{+3} , which may have R_{1e} 's much less than the reporter angular resonance frequency. The advantages of these, over spin labels, would be: (1) Their higher spin would make them more useful for determining longer distances; (2) If the chelating moiety of these modifiers

could be suitably changed to increase the off-rate of the bound relaxer paramagnetic ion, the BPR1E approach (above) could be used, allowing use of a slower shuttling system like ours. It was pointed out to us, by A. Mildvan, that metalloenzymes often have binding sites that satisfy this criterion (see Table 4 of Lin et al. 1997). The BPR1E approach (Sect “Spin labels as relaxers”) might permit useful characterization and differentiation of these sites.

Solids

Sample spinning at typical high speed will be very difficult to combine with field cycling. It may be possible to combine spinning and with shuttling, but no serious attempts have been made to do so, to our knowledge. Shuttling solids experiments using samples without spinning, with samples aligned on stacks of glass plates (Hallock et al. 2002; De Angelis et al. 2005), seem likely to be achievable, especially in a larger bore instrument, or even with a suitable probe in a 51 mm bore like ours, and a glass shuttle tube that is larger than ours, perhaps 25–30 mm inside diameter. The loose connection module would probably have to be modified to restrict the angular position of the sample as well as its coaxial and vertical positions. We think that this could be done without great difficulty.

Tumbling dampers to increase the range of applicability of internal motion studies in soluble proteins

It is often said that NMR is incapable of estimating macromolecular motions in the range of about 10^{-6} – 10^{-8} s, yet our first membrane paper (Roberts and Redfield 2004a) showed how to bridge that entire gap, as had others (Kimmich and Estaban 2004). The 10^{-8} s⁻¹ limitation occurs because this is roughly the time of rotational diffusion of typical proteins now being studied by NMR in solution, with the goal of determining of microscopic internal motion. The limitation results mainly from the fact that a motion having a time scale slower than 10^{-8} s is difficult to separate from the complete tumbling motion of the protein having roughly that time-scale or shorter (Callabero-Manrique et al. 2007). In addition, the slower internal motion is more difficult to elucidate if its amplitude is not large.

By “tumbling damper” we mean a high-molecular-weight reagent that could be added to the NMR sample at lower molarity than that of the observed protein so that the protein of interest would exist for some fraction of the time bound to the reagent, with a weak binding constant. Reporter spins on the protein would exhibit a low frequency dispersion with an inverse correlation time characteristic of the tumbling rate of the damper, or of its dissociation rate from the reporter molecule, or, preferably, of the internal dynamic rate at the reporter spin, whichever is faster. This dispersion would be

superimposed on a dispersion characteristic of the undamped tumbling of the protein of interest when it is not damper-bound. The damper might be, among many possibilities, a protein domain engineered to have the optimum dissociation rate, and engineered to be attached rigidly to a larger protein or other otherwise inert object, to increase its rotational diffusion time. The reporters might be ¹³C-enriched carbonyls on the target enzyme, as outlined above. The problem would be to engineer the damper, and then to find a concentration of it to add, to produce an observable effect without much disrupting the observation of the reporter spins.

Methods

General summary

We now turn to a description of details of improvements to our shuttler system since 2003. Much in our earlier paper (Roberts et al. 2004) is still relevant and will not be repeated. In addition, the need for some of the precautions we take is to some degree challenged by the recent paper by (Chou et al. 2011).

Installation and de-installation of our system (Fig. 1) are the reverse of each other and therefore we only mention aspects of the latter. Before de-installation the upper section (*the extender*) of the precision glass shuttle tube system, that guides the sample shuttle during its travels up and down, has to be removed. Next, the *linear motor* (Fig. 2) has to be unclamped, and pushed manually along the *rails* (towards the camera in the view of Fig. 1) to be re-clamped out of the way. Then the lower section of the shuttle tube system, that reaches from nearly the top of the commercial NMR probe up to just below the top of the rails (not visible in Fig. 1), has to be pulled out of the main magnet and the *Helmholz coils*, following which we remove the Helmholz coil assembly which sits directly on short legs that rest directly on the shell of the main magnet. A separate cooling fan for the Helmholz coils (not visible) also has to be removed. We then remove our own commercial probe, and insert the upper tube provided by Varian for sample-raising. Finally we install the community Varian probe needed for the next non-shuttling user. Our attachment does not interfere in any important way with liquid coolant filling.

Typically our shuttler remains installed for at least 2 days, during which several different samples are studied. Sample changing requires about 5 min, once the sample has been sealed into the NMR tube. We pre-seal samples into commercial NMR tubes, and cement the tubes to plastic adapters at least 8 h before use as outlined below. To remove the sample after a series of runs we disable the servomotor, uncouple the top end of the push rod from the

cross piece, and pull the long push rod, with the sample attached at its bottom, all the way out. Finally, the old sample is unscrewed from the bottom of the *loose connection module* (LCM, described below), and the next sample can be screwed on in its place prior to its insertion into the main magnet.

Linear motor and its support frame

Linear motor

The linear motor assembly is based (Fig. 2) on a servomotor and shaft driving two timing-belt pulleys that drive two side-by-side timing belts, which in turn pass over two smaller upper pulleys about 1.4 m above the motor shaft (not visible above the top of Fig. 1). The plastic cross-piece is clamped onto and between the two belts, and the rotary motor is programmed by the microprocessor to move it at high speed, up to 10 m/s, a distance of up to 883 mm above the sensitive region of the main magnet, and later back, as specified and executed by commands from the spectrometer's computer (see below). These components are mounted permanently (except for maintenance and repair) on a heavy base to which is attached a vertical post projecting upward to hold the two upper pulleys. This assembly can be loaded, when necessary, by the installer alone (often this writer), onto the front part of the frame using a human-powered fork-lift (not described here).

The servomotor is precision-mounted on one of the end plates of the base. A stainless steel shaft is connected to the motor by a rigid coupling (a flexible coupling should not be used, it de-stabilizes the servomotor!). Timing pulleys (40 teeth HTD5) are mounted on the shaft with special no-slip clamps. The two timing belts, 9 mm wide, pass over smaller pulleys (not shown) above the magnet on the strong vertical post that is fastened to the backplane. These upper pulleys each exert a force on one of the belts of about 10 Kgf per pulley, determined by a system of cables, springs, and a single adjusting turnbuckle.

The motor is an integrated-control servomotor (MAC 400, JVL, Demark), operated in a stepper-motor-emulation mode. The motor overshoots momentarily at the end of the fast motion, but overshoot is less than 5 mm for a few ms, and is of no consequence because of our use of the LCM (described below) to connect the push rod to the sample. The maximum acceleration/deceleration of the sample during travel is about 20 times the free gravitational acceleration at the earth's surface.

Frame

The frame is a tall table-like structure constructed of 38 mm standard aluminum angle stock, which surrounds

the main magnet without touching it. Its main function is to support the two top rails on which the motor assembly sits. Each of these rails is heavy aluminum angle stock, covered on top with strips of Teflon to permit easy sliding of the motor. The distance between the rails is 19.5 cm.

We intentionally did not attempt to make the frame transversally rigid, although vertically it is. Instead, the whole apparatus has two major almost separate domains, one being the frame, linear motor, push rod, and upper part of the flexible coupling module between the push rod and sample; and the other being the main magnet and a few other parts of the system supported by it, such as the glass shuttle tube and the Helmholtz coils. When the sample is in its readout position at the main magnet center, these two collections of components are coupled together only very weakly by slight friction of the upper flexible coupling with the glass shuttle tube, by the very flexible hula coupling, and also by a compromise we made with the vibration-tolerant principle just enunciated, motivated by the desirability to keep the top of the frame located so that the pushrod top is centered within about 1.5 mm above the hula bearing center. We help assure this by means of a light-weight cushioned transverse coupling between the upper frame and the magnet top, based on four horizontal lightweight clamps (Fisher 05-769-6Q), mounted onto the bottoms of the rails, and each grasping one of four rigid vertical rods that we connected rigidly to the shipping tabs on the top of the main magnet.

Sample tubes, longitudinally loose connection module (LCM) and push rod

Sample tubes and sample changing

About at least 8 h or more before each run, each sample is sealed with household epoxy cement, at the bottom of an 89 mm-long standard commercial 8 mm NMR tube (Wilmad 513A-5PP-3.6) or a similarly shortened tube, under a 43 mm long hollow plastic plug, that was pushed and cemented inside the NMR tube above the liquid sample. As described in Fig. 4c of (Redfield 2003), the purpose of this hollow plug is to eliminate bubbles that might appear in the sample region and destroy the resolution; and also to serve as a top susceptibility-match plug.

Twenty minutes or more after the above sealing procedure, we epoxy-cement the top end of the NMR tube into a 5 cm long PEEK adapter, with the aid of a massive V-block for alignment, while the epoxy sets. After 6 h or more this assembly is ready to be inserted into the shuttler.

Loose connection module (LCM)

It connects the push rod (below) with the plastic adapter into which is cemented the short NMR tube. The LCM by

itself allows the NMR tube to move freely vertically only about 9 mm relative to the push rod, while at the same time keeping it pointed precisely downward so that it does not contact the internal components of the commercial probe when it moves down into it. It consists of two major parts, each made from several polyetheretherketone (PEEK) pieces that are epoxy-cemented or screwed together (Fig. 5) The lower part of the LCM resembles the previous freely-moving shuttle (Redfield 2003) in that the NMR sample is screwed into its bottom end (via the adapter), and it has two precisely-machined cylindrical ridges on the top and bottom of its outer surface, to guide the NMR tube into the probe's entry hole without touching the latter.

The upper part of the LCM likewise has two such cylindrical surfaces on discs at its upper end, and is semipermanently connected, by a screw, to the bottom end of the push rod.

These two parts both slide separately inside the precision glass shuttle tube. They are trapped together by a disc on the end of a smaller (6.3 mm diameter) rod capped at its bottom by a 9.5 mm diameter disc, held onto the central rod of the upper part of the LCM by a screw. Further details about the LCM are given in Fig. 5 and its caption.

In order to define the vertical position of the sample during both the FID and the prior relax-time, we apply air pressure or suction through a side tube at the top of the shuttle tube, of magnitude ~ 0.2 bar. Dry-air pressure is applied starting from the time when the servomotor starts to move the sample downward, and is switched to suction at the start of the upward motion, by solenoid valves controlled by the microprocessor.

Push rod and Hula bearing

The LCM is semi-permanently screwed into the short lower cylindrical brass end-piece cemented onto the push rod. The latter is a carbon-composite tube 7.9 mm in diameter, 114 cm long (On-Line metals) whose similarly cemented upper cylindrical brass end piece is easy for the user to couple to the center of the horizontal *cross piece* that connects the two timing belts of the linear motor. Trapped between these brass end pieces, and sliding freely on the push rod, is the upper part of the *Hula bearing*. It allows free vertical passage of the push rod, with some freedom of sideways motion, into the inside of the glass shuttle tube, without serious loss of the air pressure or suction mentioned just above. It consists of a Teflon sleeve 2 cm long with a central hole whose inside diameter is ~ 0.5 mm larger than the outside diameter of the push rod. It is clamped to the upper end of a short piece of a ~ 5 cm long gum rubber tubing.

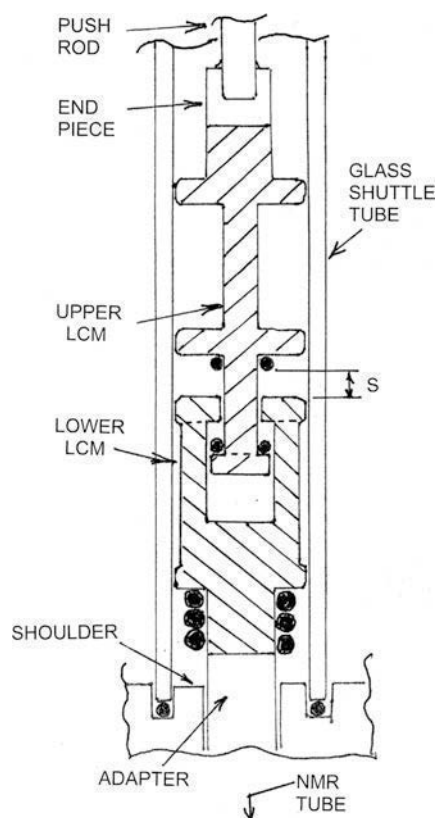


Fig. 5 Cartoon of the loose connection module (LCM) that couples vertical motion of the push rod to the sample. Only the parts of the LCM itself are cross-hatched, and differently for its upper and its lower parts. The NMR sample tube (not shown) is screwed into the lower part of the LCM via a 5 cm-long adapter, to which it is cemented before each cycling run. The upper part of the LCM is attached semi-permanently to the push rod which extends up about 1 M to the cross bar connecting the two belts (see Figs. 1, 2). When the sample-LCM-push-rod combination is assembled and inserted into the glass shuttle tube, the two cross hatched parts of the LCM are each precisely constrained to be coaxial with the glass tube. The distance, labeled S in the figure, can vary from zero to 9 mm when the assembly is not at the bottom of its travel. During the relax-time, the servomotor is programmed to hold the push rod lower end at a point, typically many cm above the probe, and suction from the top pulls the two parts of the LCM together so that S is zero. During the readout part of the cycle, the lower part of the LCM contacts a circular shoulder which is part of the lower support of the glass tube, and is attached to the heavy brass tube connected, ultimately, to the main magnet. During this time mild air pressure is applied from the top, to assure that the lower part of the LCM does, in fact, rest firmly on the shoulder. The sample and adapter extend through the central hole of the shoulder, the former into the probe itself; and the motor is programmed to make the spacing S to be about 2 mm, so that the upper part of the LCM can vibrate and overshoot slightly, vertically, without touching the lower part. The upper and lower parts of the LCM are each made from several pieces of PEEK cemented together. *Dotted lines* within them indicate where they can be partly disassembled for inspection. Machine screws that hold these and other components together, that are not cemented, are not shown. *The solid circles* are O-ring cushions. Radial slots (not shown) are machined into the discs of the upper part of the LCM, to allow the pressure or vacuum, introduced from the top of the shuttle tube, to reach the top of the lower part of the LCM

Glass shuttle tube system, and room temperature coils

Shuttle tube extender

Its metal outer support holds the upper section of the glass shuttle tube (visible in Fig. 1) The entire extender assembly has to be removed to allow the linear motor to slide past on the rails during installation. It is needed to provide space for the LCM to occupy, when the sample is at its highest point 65 mm above the top flange of the main magnet. It extends upward 25 cm from just below the top surface of the rails.

Its top aluminum part holds the lower half of the top quick-disconnect fitting, through which passes the push rod. The upper half of this fitting holds a 16 mm outside-diameter tube, to which is clamped the gum-rubber tube that is the stomach of the Hula bearing.

The top of the extender also has a side-arm for introduction of the approximately 0.2 bar of dry air pressure, or suction, used to enforce the desired state of extension of the LCM, as mentioned above.

The bottom end of the extender has a flange, which is clamped to the top ring of the lower long glass shuttle tube module, by quick-disconnect finger clamps. The inside diameter parts of the connection between the two glass parts must be well aligned concentrically. The outer diameter of the glass tube supplied by Wilmad is not precision-made, only the inside is. We have devised a way to epoxy-cement short cylindrical pieces of plexiglass on the ends of these glass tubes so that the precision-made outer surfaces of the plastic are precisely concentric with the inside diameter of the glass. The plastic outer surfaces can then be held precisely and concentrically without special adjustments, to allow us to routinely design precision mountings between the tube ends.

Long glass shuttle tube assembly

Its top is a strong plastic (Noryl) annular disc (barely visible in Fig. 1) which extends over the top of the Helmholtz coil assembly, and it has three 9 mm long bottom legs which sit on the Helmholtz assembly and support the rest of the shuttle tube assembly from above. Machined into its top is the lower half of the coupling to the extender module. This top disc is connected, by aluminum brass rods extending downward 11 cm, to a smaller annular plate that fits inside the centers of the Helmholtz coils, and is about 1 cm above the top flange of the main magnet. This plate is, in turn, soldered to a long (72 cm) heavy brass tube that extends nearly down to the top of the commercial NMR probe.

The upper part of the long glass shuttle tube, between the two discs just mentioned, is not covered by metal but is

surrounded by the fast-switching coil, wound on a close-fitting light plastic form. This coil is centered on the point 65 mm above the main magnet's top flange where the sample is stopped for relaxation studies at or below 0.065 T.

Room temperature coils

The Helmholtz coils are fan-cooled. The currents in their windings are programmed to cancel the first-order gradient of about two mT per cm from the main magnet at the point 65 mm above the main magnet flange, while varying the field there from 0.015 to 0.08 T (not including the extra contribution discussed in the next paragraph). These coils are turned off when they are not needed to avoid overheating.

The fast-switching coil mentioned above is 3 layers of heavy copper wire, 3 cm inside diameter and 5 cm long, which provide 0.015 T of additional magnetic field. This field can be reversed electronically in a few ms. Together with the Helmholtz pair, it can thus perform a combined mechanical/switched-magnet shuttle down to between 0.065 and zero T in two stages, with the last stage taking a few ms to jump the field by 0.03 T. This capability is useful for vesicle samples for which R_1 usually increases below about 0.05 T (Fig. 3b).

Electronics, pulse sequences, and operation

Processors

The system is run by a 16-bit microprocessor (Microchip Explorer 16), and a simple parallel interface that we built to monitor or control the ~25 I/O lines of the equipment's hardware. It also receives real-time 16-bit instructions from the Varian console via the latter's rear console 25 pin interface connector, as initiated by a strobe pulse from one of the Varian's spare pulse output coax connectors. This strobe triggers an interrupt-service routine of the microprocessor, which then performs the function encoded in the instruction. We have to insert relatively short sections of instruction code into pulse-sequence listings from the Varian library, to make the microprocessor act as needed at the proper time. Some of these instructions initialize variables during the nuclear spin polarization recovery time, and others signal the microprocessor to execute real-time actions during the sequence such as turning on/off magnetic fields at appropriate times, or moving the sample up or down. As a result it is easy to make these additions to standard pulse sequence listings because they are bunched into a few blocks that can be used for any cycling application, and in the future we can paste them at appropriate places into a pre-existing non-cycling code sequence

without much extra modification. The microprocessor also communicates error codes to a low-end personal computer (PC) in the console, for display of appropriate user-directed messages on its screen. The PC is also used for software development and debugging, and to set up the integrated control system contained within the servomotor using software supplied with it.

The field, at which the sample is to relax during each run (we use “run” to mean “experiment” in Varian and Bruker terminology), is entered as a parameter by the operator, and the Varian’s computer calculates (among other things) how many mm the sample must be moved, with one mm resolution, to reach this field.

Pulse sequences

We have adapted sequences to performed two different experiments: (1). 1D R_1 measurement of ^{31}P and of enriched ^{13}C using direct observation; and (2). 2D R_1 measurement on ^{15}N by the standard HSQC-based method. In general the final spin polarizations are likely to be severely relaxed by the cycling process, so that flip-back methods of solvent nuclear-spin polarization conservation are useless. Instead we start unconventionally with a purge sequence for the observed nucleus for the direct observe one-dimensional experiment, or for protons for the two-dimensional sequence. The purge is a 90° pulse followed by another one shifted 90° . This is followed by a 1.5–4 s recovery time to give a reproducible starting polarization.

The 2D sequence is based on the $g\text{Nhsqc}$ sequence in the Varian library. As expected, solvent H_2O phase-noise was potentially more of a problem for this proton-readout sequence despite use of the now-standard gradient-based methods for its elimination, but was acceptable because the phase-noise was at the solvent frequency.

The relax-time, in the original 2D library sequence, is replaced by us with a shuttle-upward (to a lower field), followed by the relax-time delay (arrayed as usual in a series of sub-runs all at the same field), and shuttle downward, back to the 11.7 T field at the center of the main magnet. For the 1D direct observation runs, the shuttle-relax-shuttle was directly preceded by two 90° pulses at the reporter frequency, one fixed in phase and the other cycled alternately by 180° , with in-step 180° cycling of recording, to eliminate, primarily, proton-to- ^{31}P NOE. The latter is of interest, however, and we expect to be able to observe proton-to- ^{31}P NOE by instead applying the two 90° pulses, just before the shuttling, at the proton frequency.

For relax-time fields of less than 0.55 T, where the sample was always moved to 65 mm above the main magnet flange, the room-temperature coils were turned on with sufficient advance turn-on time, to be at field during the relax-time.

Operation

Individuals with only experience with conventional NMR have easily learned to use the system. As already mentioned, many hours, preferably the day before running, the sample has to be sealed into a short 5 or 8 mm NMR tube which is then cemented into a plastic adapter. The writer often does this, but the procedure is very simple and could be learned by any heavy user. The user can also learn how to change samples in our system, or be given help in doing so, and has to enter the relaxing magnetic field into the computer to be used for each run, and the usual array of relax-time delays, in the way provided by Varian. We commonly program a series of queued runs lasting overnight or more, each at a different field, and a different set of arrayed relax-times. Analysis is the user’s problem, and our approach to it is described in some of our papers.

Conclusions

Our most significant accomplishment has probably been simply to show that such a shuttler can be used in conjunction with a commercial spectrometer without modification of the latter. The entire system can be installed de novo onto the spectrometer, or the reverse, in about 1 h. It can also be left partly installed without interference with the intended routine use of the spectrometer, and fully reinstalled in slightly more time than needed for a probe change. In the 8 + million reciprocations of the device we have had only one that required probe rebuilding. Thus, the natural fear that such a system would destroy probes is dispelled to a considerable degree.

As a result we have capability unmatched elsewhere, with many applications that we have not been able to try. The capability is so great, and unconventional, that we do not think of novel applications until well after starting work on some new kinds of problems. Major new applications could be to interactions between macromolecules, and to studies of larger complexes using smaller reporter species.

The design as it stands would be compatible with any commercial spectrometer, by use of relatively simple modifications. In this article we have, for the most part, documented what we have done without much discussion of other approaches, such as the novel new approach of (Chou et al. 2011). The shuttler is intended primarily as a short-term small-scale upgrade of the now-fully-developed technology of high-resolution NMR in liquids, as opposed to a dramatic long-range meta-development, such as DNP.

The present article is meant to encourage the proliferation of devices like ours into other NMR laboratories, as well as to documentation of methods used in our previous experiments. We will not be able investigate further

significant improvements on our instrument and methods, and we look forward to efforts by others to demonstrate similar or alternative approaches.

Acknowledgments This development was supported by National Institutes of Health grant GM077974, and, previously, grant CHE-0109575 from the National Science Foundation Chemical Instrumentation Program, and grant 36680-ACF from the American Chemical Society Petroleum Research Fund. Marcel Reese suggested the use of a servomotor, and its supplier, for this device. We thank our research collaborators, especially Mary Roberts, for performing much of the research reviewed here, and helping prepare the figures. David Roberts provided the photographs, and Thomas Pochapsky kindly read this manuscript. We received much technical help from many individuals in building this shuttler, especially from Frank Mello who fabricated parts for us as well as providing many useful suggestions, and Annemarie Rom-Weisenbach for expert programming. We thank Tai-huang Huang for sending us the recent paper describing the new shuttle design (Chou et al. 2011).

References

- Amero C, Schanda P, Ascunson Dur A, Iyala I, Marion D, Franzetti B, Brutscher B, Boisbouvier J (2009) Fast two-dimensional NMR spectroscopy of high molecular weight assemblies. *J Am Chem Soc* 131:3448–3449
- Batnagar J, Borbat P, Pollard A, Bilwes A, Freed J, Crane B (2010) Structure of the ternary complex formed by a chemotaxis receptor signaling domain, the CheA histidine kinase, and the coupling protein CheW as determined by pulsed ESR spectroscopy. *Biochemistry* 49:3824–3841
- Borbat P, Freed J (2007) Measuring distances by pulsed dipolar ESR spectroscopy: spin-labeled histidine kinases in two component signaling systems. In: Simon M, Crane B, Crane A (eds) *Methods in enzymology*, vol 423. Elsevier, pp 52–116
- Brown M, Ribiero A, Williams G (1983) New view of lipid bilayer dynamics from ^2H and ^{13}C NMR relaxation time measurements. *Proc Natl Acad Sci USA* 80:4325–4329
- Callabero-Manrique E, Bray J, Deutschman W, Dahlquist F, Guenza M (2007) A theory of protein dynamics to predict NMR relaxation. *Biophys J* 93:4128–4140
- Chou C-Y, Chu M, Chang C-F, Huang T-h (2011) A compact high-speed mechanical sample shuttle for field-dependent high-resolution solution NMR. *J Magn Reson*. doi:10.1016/j.jmr.2011.12.001
- Clarkson M, Lei M, Eisenmesser E, Labeikovsky W, Redfield A, Kern D (2009) Mesodynamics in the SARS nucleocapsid measured by NMR field cycling. *J Biomol NMR* 45:217–225
- Clore M, Gronenborn A (1982) Theory and applications of the transferred nuclear Overhauser effect to the study of the conformations of small ligands attached to proteins. *J Magn Reson* 48:402–417
- Clore M, Iwahara J (2009) Theory, practice, and applications of paramagnetic relaxation enhancement for the characterization of transient low-population states of biological macromolecules and their complexes. *Chem Rev* 109:4108–4139
- Da Costa G, Mouret L, Chevanc S, Le Rumeur E, Bondon A (2007) NMR of small molecules interacting with lipids in small unilamellar vesicles. *Eur Biophys J* 36:933–942
- De Angelis A, Jones D, Grant C, Park S, Mesleh M, Opella S (2005) NMR experiments on aligned samples of membrane proteins. In: James T (ed) *Methods in enzymology*, vol 394. Elsevier, pp 350–382
- Diakova G, Goddard Y, Korb J-P, Bryant R (2010) Water and backbone dynamics in a hydrated protein. *Biophys J* 98:138–146
- Dolainski C, Unger M, Bloom M, Bayerl T (1985) Two-dimensional exchange ^2H NMR experiments of phospholipid bilayers on a spherical solid support. *Phys Rev E* 51:4743–4750
- Ferrante G, Sykora S (2004) Technical aspects of fast field cycling. In: van Edik R, Bertini I (eds) *Advances in inorganic chemistry*, vol 57. Academic Press, pp 405–470
- Gaede H, Gawrisch K (2003) Lateral diffusion of lipid, water, and a hydrophobic drug in multilamellar liposomes. *Biophys J* 85:1734–1740
- Grosse S, Gubaydullin F, Scheelken S, Vieth H-M, Yurkovskaya A (1999) Field cycling by fast NMR probe transfer: design and application in field-dependent CIDNP experiments. *Appl Magn Reson* 17:211–225
- Gueron M (1975) Nuclear relaxation in macromolecules by paramagnetic ions: a novel mechanism. *J Magn Reson* 19:58–66
- Hallock K, Wildman K, Lee D-K, Ramamoorthy A (2002) An innovative procedure using a sublimable solid to align bilayers for solid-state NMR studies. *Biophys J* 82:2499–2503
- Hecht R, Redfield A (1963) Overhauser effect in metallic lithium and sodium. *Phys Rev* 132:972–977
- Ivanov D, Redfield A (2004) Field cycling method with central transition readout for pure quadrupole resonance detection in dilute systems. *J Magn Reson* 166:19–27
- Kang C, Vanoye C, Welch R, Van Horne W, Sanders C (2010) Functional delivery of a membrane protein into oocyte membranes using bicelles. *Biochemistry* 49:632–655
- Kerwood D, Bolton P (1987) A sample shuttling device suitable for two-dimensional low-field NMR. *J Magn Reson* 75:142–146
- Kimmich R, Estaban A (2004) Field cycling NMR relaxometry. *Prog NMR Spectrosc* 44:257–320
- Klauda J, Eldho N, Gawrisch K, Brooks B, Pastor R (2008a) Collective and noncollective modes of NMR relaxation in lipid vesicles and multilayers. *J Phys Chem B* 112:5924–5929
- Klauda J, Roberts M, Redfield A, Brooks B, Pastor R (2008b) Rotation of lipids in membranes: MD simulation, ^31P spin-lattice relaxation, and rigid-body dynamics. *Biophys J* 94:3074–3083
- Koenig S, Brown R (1990) Field cycling relaxometry of protein solutions and tissues: implications for MRI. *Prog NMR Spectrosc* 22:487–567
- Korchak S, Kiryutin A, Ivanov K, Yurkovskaya A, Grishin Y, Zimmermann H, Vieth H-M (2010) Low-field, time-resolved dynamic nuclear polarization with field cycling and high-resolution NMR detection. *Appl Magn Reson* 37:515–537
- Krahn A, Lottman P, Marquardsen T, Tavernier A, Turke M-T, Reese M, Leonov A, Bennati M, Hofer P, Engleke F, Griesinger C (2010) Shuttle DNP spectrometer with a two-center magnet. *Phys Chem Chem Phys* 12:5830–5840
- Lane AN, Jenkins T, Brown T, Neidle S (1991) Interaction of beneril with the *EcoRI* dodecamer d(CGCGAATTCGCG) $_2$ in solution studied by NMR. *Biochemistry* 30:1372–1385
- Leftin A, Brown M (2011) An NMR database for simulations of membrane dynamics. *Biochem Biophys Acta* 1808:818–839
- Leggett J, Hunter R, Granwehr J, Panek R, Linde A, Horsewill J, McMaster J, Smith G, Kockenberger W (2010) A dedicated spectrometer for dissolution DNP NMR spectroscopy. *Phys Chem Chem Phys* 12:5883–5892
- Lin J, Abaygunawardana C, Frick D, Bessman M, Mildvan A (1997) Solution structure of the quarternary Mut-T-M $^{2+}$ complex and mechanism of its pyrophosphohydrolyase reaction. *Biochemistry* 36:1199–1211
- Lurie D, Aime S, Baroni S, Booth N, Broche L, Choi C-H, Davies G, Ismail S, ÓhÓgain D, Pine K (2010) Fast field-cycling magnetic resonance imaging. *Compt Rend Physique* 11:136–148
- Palmer AG III (1997) Probing molecular motion by NMR. *Curr Opin Struct Biol* 7:732–737

- Pileio G, Carravata M, Levitt M (2010) Storage of nuclear magnetism as long-lived singlet order in low magnetic field. *Proc Natl Acad Sci USA* 107:17136–17139
- Pu M, Fang X, Gershenson A, Redfield A, Roberts M (2009a) Correlation of vesicle binding and phospholipid dynamics with phospholipase C activity: insights into phosphatidylcholine activation and surface dilution inhibition. *J Biol Chem* 284:16099–16107
- Pu M, Feng J, Redfield A, Roberts M (2009b) Enzymology with a spin-labeled phospholipase C: soluble substrate binding by ^{31}P NMR from 0.005 to 11.7 Tesla. *Biochemistry* 48:8282–8284
- Pu M, Orr A, Redfield A, Roberts M (2010) Defining specific lipid binding sites for membrane-bound phospholipase C, by ^{31}P NMR from 0.005 to 11.7 T. *J Biol Chem* 285:26916–26922
- Raschle T, Hiller S, Etzkorn M, Wagner G (2010) Nonmicellar systems for solution NMR spectroscopy of membrane proteins. *Curr Opin Struct Biol* 20:471–479
- Redfield A (2003) Shuttling device for high-resolution measurements of relaxation and related phenomena in solution at low field, using a shared commercial 500 MHz NMR instrument. *Magn Reson Chem* 41:753–768
- Roberts M, Redfield A (2004a) High-resolution ^{31}P field cycling NMR as a probe of phospholipid dynamics. *J Am Chem Soc* 126:13765–13777
- Roberts M, Redfield A (2004b) Phospholipid bilayer surface configuration probed quantitatively by ^{31}P field-cycling NMR. *Proc Natl Acad Sci USA* 101:17066–17071
- Roberts M, Cui Q, Turner C, Case D, Redfield A (2004) High-resolution field-cycling NMR studies of a DNA octamers as a probe of phosphodiester dynamics and comparison with computer simulation. *Biochemistry* 43:3637–3650
- Roberts M, Mohanty U, Redfield A (2009) Phospholipid reorientation at the lipid/water interface measured by high resolution field cycling ^{31}P NMR spectroscopy. *Biophys J* 97:132–141
- Shi X, Shao C, Zhang X, Zambonelli C, Redfield A, Head J, Seaton B, Roberts M (2009) Modulation of *Bacillus thuringiensis* phosphatidylinositol-specific phospholipase C activity by mutations in the putative dimerization interface. *J Biol Chem* 284:15607–15618
- Sivanandam V, Cai J, Redfield A, Roberts M (2009) Phosphatidylcholine “wobble” in vesicles assessed by high-resolution ^{13}C field cycling NMR spectroscopy. *J Am Chem Soc* 131:3420–3421
- Sousa D, Fernandes G, Marques G, Ribiero A, Sebastiaou P (2004) Novel pulsed switched power supply for a fast field cycling NMR spectrometer. *Solid State NMR* 25:160–166
- Strombotne R, Hahn E (1964) Longitudinal nuclear spin–spin relaxation. *Phys Rev A* 133:1616–1629
- Victor K, Kavolius Y, Bryant R (2004) Magnetic relaxation dispersion probe. *J Magn Reson* 171:253–257
- Victor K, Van-Quynh A, Bryant R (2005) High frequency dynamics in hemoglobin measured by magnetic relaxation dispersion. *Biophys J* 88:443–454
- Wang Y, Chen W, Blair D, Pu M, Xu Y, Miller S, Redfield A, Chiles T, Roberts M (2008) Insights into the structural specificity of the cytotoxicity of 3-deoxy-phosphatidylinositols. *J Am Chem Soc* 130:7746–7755
- Weitekamp DP, Zax D, Zilm K, Pines A (1983) Zero field magnetic resonance. *Phys Rev Lett* 50:1807–1810